IOPscience iopscience.iop.org

Home Search Collections Journals About Contact us My IOPscience

Self-consistency in total energy calculations: implications for empirical and semi-empirical schemes

This article has been downloaded from IOPscience. Please scroll down to see the full text article.

1991 J. Phys.: Condens. Matter 3 8351

(http://iopscience.iop.org/0953-8984/3/43/003)

View the table of contents for this issue, or go to the journal homepage for more

Download details:
IP Address: 171.66.16.159
The article was downloaded on 12/05/2010 at 10:37

Please note that terms and conditions apply.

J. Phys.: Condens. Matter 3 (1991) 8351–8367. Printed in the UK

Self-consistency in total energy calculations: implications for empirical and semi-empirical schemes

I J Robertson, M C Payne and Volker Heine
Cavendish Laboratory, Madingley Road, Cambridge CB3 0HE, UK

Received 4 July1991

Abstract. We assess the viability of non-self-consistent total energy calculations using the Harris–Foulkes energy functional. The self-consistent electron density in 11 aluminium structures is resolved into components that are qualitatively similar to the free pseudo-atomic density. For many of the structures the components display significant anisotropies, whilst between the structures there are also important differences. By studying the sensitivity of the Harris–Foulkes energy functional to perturbations in the input electron density, we are able to relate these differences in atomic-like densities to differences in energy. We conclude that no estimate for the electron density based on the superposition of spherical densities can be expected to give errors in the energy of less than 0.03 eV per atom. Given the significant variation in atomic-like electron densities from structure to structure, any transferable density scheme is also prone to energy errors. By constructing a least-squares fit of our electron density data to a given functional form, we conclude that the errors in the absolute energies per atom are typically of the order of 0.05 eV whilst for energy differences they drop to 0.01 eV.

1. Introduction

The development of ever more efficient algorithms and access to ever more powerful computers has allowed the *ab-initio* simulation of progressively larger and more complicated condensed matter systems [1]. In spite of this progress there are still many situations in which an *ab-initio* approach is not feasible. The calculation of total energies and hence the simulation of such systems is only possible by the use of empirical and semi-empirical schemes [2–7].

Nowadays most *ab-initio* total energy calculations are carried out within the density functional formalism [8], using a local approximation to the exchange–correlation energy. As the name suggests, within this formalism, it is the electron density which plays a central role. For a given input density, a Hamiltonian is constructed. Output eigenvalues, wavefunctions and electron densities are calculated. An estimate for the energy is then given by the Kohn–Sham functional, which is a sum of the occupied eigenvalues and a number of terms dependent on both the input and output electron density. Better results may be obtained using the output density as the input for the next cycle and iterating towards convergence. For the correct input electron density the functional is stationary, a local minimum, and gives the correct energy of the system. For this same density the input and output densities are equal, and are said to be self-consistent. If the energy is evaluated near but not at the self-consistent electron density then only second-order errors in the energy will result. However, given

0953-8984/91/438351+17$03.50 © 1991 IOP Publishing Ltd

the high degree of reliability of the other aspects of these calculations, one generally iterates very near to the true ground state density. For this reason these calculations are generally self-consistent.

Electron density is equally important in many empirical and semi-empirical schemes. In the embedded atom method [4], the effective medium method [2] and the glue model [3], the energy of a given atom is determined by the electron density it feels from its neighbours. In the many-atom bond order potential model [5], the strength of a bond is determined by its environment which, in turn, is determined by the electron densities of its neighbours. Foulkes and Haydock [9] have shown that even in the semi-empirical tight-binding model [7], the form of the energy may be derived from suitable assumptions about the nature of the electron density.

Although central to all schemes, the treatment of the electron density does of course differ significantly between self-consistent schemes, and the other methods. In the former, the electron density used to evaulate the energy is essentially correct and of no pre-supposed form. In the latter the electron density used is not exact and is constrained to be comprised of atomic-like, spherical electron densities centred on the nuclei which make up the system. The relative success of empirical and semi-empirical schemes suggests that this assumed form of the electron density may in fact be reasonable.

Motivated by this observation and using an alternative energy functional, firstly Harris [10] and then, independently, Foulkes and Haydock [9] have proposed a new method for non-self-consistent total energy calculation. The self-consistent electron density is approximated by superposition of atomic-like densities. A corresponding electronic potential and Hamiltonian are generated. Occupied eigenvalues of the Hamiltonian are found and summed over, and various other energy terms depending only on the explicit input electron density are calculated. All the terms are added together to give an estimate of the total energy which depends only on the input electron density. The output electron density is never calcualed.

The ideas of Harris, Foulkes and Haydock have been investigated by Read and Needs [11] and by Finnis [12]. Read and Needs have studied the performance of the Harris–Foulkes functional for bulk and for surfaces of silicon and aluminium using a superposition of pseudo-atomic densities. They have found that for bulk structures the functional does well. However, for surfaces, the functional performs less well. Finnis has performed similar calculations, and obtained similar results. It had been postulated that the Harris–Foulkes functional displayed a local maximum around the self-consistent density. On the basis of this, Finnis tried to optimize the atomic-like densities he superimposed, so as to maximize the value of the Harris–Foulkes functional. It is now known [13] that the functional is in fact either a local minimum or a saddle-point, and hence this procedure must be considered invalid.

The main aim of this paper is to attain an understanding of the nature of the self-consistent electron density in a wide range of aluminium structures. We wish to understand the extent to which it may be considered to be a superposition of atomic-like densities, to what extent these densities are spherically symmetric, their relationship to the true pseudo-atomic density and the extent to which they are transferable from structure to structure.

The purpose of our work is threefold. Firstly we wish to understand the magnitude of self-consistency effects. In this way we may appreciate the limitations of those empirical and semi-empirical schemes which ignore [3–6] or approximate them [2]. Secondly we wish to explore the possibility of performing accurate non-self-consistent

total energy calculations. That is, can we, for any structure, write down *a priori* a good approximation to the self-consistent electron density, avoiding the need for time-consuming iterations to self-consistency? Finally, in obtaining transferable atomic-like densities we would have the ingredients for a quick, approximate, but non-empirical total energy scheme.

The outline of the paper is as follows. In section 2 we calculate the self-consistent charge density of a number of aluminium structures. We explore the possibility of resolving these charge densities into localized components. We study the differences between these localized distributions and the true pseudo-atomic electron density. In section 3 we study the sensitivity of the Harris–Foulkes energy functional to errors in the input charge density. In section 4 we use the results of sections 2 and 3 to deduce some bounds on the reliability of any non-self-consistent schemes. We conclude in section 5 with a summary of our results and the direction of our future work.

2. The self-consistent charge density

2.1. Computational details

The first step of our work is to choose those aluminium structures that we wish to study. Since one of our motives for this study is as part of an on-going investigation of many-atom bonding in metals, it is natural that we use those structures which we have already studied in an alternative context [14]. All of these structures are periodic. Details of the unit cells, whose axes are mutually orthogonal, are given in table 1. All these structures have an atomic nearest neighbour separation of 2.85 Å but differ in coordination number, with values ranging from 0 for our atomic structure to 12 for the FCC structure.

For each structure we generate the self-consistent electron density. We use a Car–Parrinello algorithm [15], expanding the wavefunctions in a plane wave basis with a cut-off energy of 190 eV. To represent the ions we use a local pseudopotential of the Heine–Abarenkov type [16,17] and for exchange-correlation we use the function of Ceperley and Alder [18] as parametrized by Perdew and Zunger [19]. Many of our structures are metallic, which implies a need for a large number of k-points. In order to achieve this cheaply, we use the $\boldsymbol{k}\cdot\boldsymbol{p}$ method [20], and solve over an $8 \times 8 \times 8$ Monkhorst–Pack grid of k-points [21].

2.2. Resolution into atomic-like components

Consider a periodic system of N identical atoms whose nuclei are at positions $\boldsymbol{R}_i$. By identical we mean not only that the atomic species are identical, but also that the environment of each atom is identical. We may formally write the self-consistent charge density $\rho(\boldsymbol{r})$ of this system as a superposition of identical components. In anticipation of the form of these components, we will refer to them as atomic-like components of ALDs, and represent them by the sympol ρ_{ALD}:

$$\rho(\boldsymbol{r}) = \sum \rho_{\mathrm{ALD}}(\boldsymbol{r} - \boldsymbol{R}_i)\,. \tag{1}$$

Taking the Fourier transform of (1) we have for each reciprocal lattice vector of our system

$$\rho(\boldsymbol{G}) = \rho_{\mathrm{ALD}}(G)S(\boldsymbol{G})/V \tag{2}$$

Table 1. Lattice parameters and atomic coordinates for the 11 aluminium structures.

Structure	a (Å)	b (Å)	c (Å)	Atomic coordinates
FCC	4.0305	4.0305	4.0305	(0.00, 0.00, 0.00) (0.50, 0.50, 0.00) (0.50, 0.00, 0.50) (0.50, 0.50, 0.50)
Vacancy lattice	4.0305	4.0305	4.0305	(0.50, 0.50, 0.00) (0.50, 0.00, 0.50) (0.50, 0.50, 0.50)
Simple cubic	2.8500	2.8500	2.8500	(0.00, 0.00, 0.00)
Diamond	6.5817	4.6540	4.6540	(0.00, 0.00, 0.00) (0.25, 0.50, 0.00) (0.50, 0.50, 0.50) (0.75, 0.00, 0.50)
Atom	5.7000	5.7000	5.7000	(0.00, 0.00, 0.00)
Line	2.8500	5.7000	5.7000	(0.00, 0.00, 0.00)
Square lattice	2.8500	2.8500	5.7000	(0.00, 0.00, 0.00)
Close-packed layer	2.8500	4.9363	5.7000	(0.00, 0.00, 0.00) (0.50, 0.50, 0.50)
Square slab	8.5500	2.8500	2.8500	(0.00, 0.00, 0.00) (0.33, 0.00, 0.00)
FCC slab	7.3471	4.0305	4.0305	(0.00, 0.00, 0.00) (0.27, 0.50, 0.00) (0.27, 0.00, 0.50) (0.00, 0.50, 0.50)
Graphite	5.7000	8.5500	4.9363	(0.00, 0.00, 0.00) (0.00, 0.33, 0.00) (0.00, 0.50, 0.50) (0.00, 0.83, 0.50)

where $S(\boldsymbol{G})$ is the structure factor and V is the volume of the unit cell. For those values of $\boldsymbol{G}$ for which $S(\boldsymbol{G})$ is not zero, we then have

$$\rho_{\mathrm{ALD}}(\boldsymbol{G}) = \rho(\boldsymbol{G})V/S(\boldsymbol{G})\,. \tag{3}$$

At first glance, the information furnished by equation (3) regarding the ALD for this structure is rather restricted. In particular, it is limited to that finite number of reciprocal lattice vectors, $\boldsymbol{G}$, consistent with the periodicity of the structure, and for which $S(\boldsymbol{G})$ is not zero. This is not a problem. One may always consider a structure as being comprised of large supercells whose dimensions are multiples of the dimensions of the original unit cell. The values of $\boldsymbol{G}$ consistent with this new cell will then be more densely distributed in reciprocal space. However, the structure factor corresponding to those new values of $\boldsymbol{G}$ will necessarily be zero and equation (3) cannot be employed. To overcome this problem we displace the atoms of our supercell by a very small amount. Given that the environment of each atom has been barely modified we may still assume that all atoms are equal. (The validity of this assumption is addressed in section 2.5.) The function $\rho_{\mathrm{ALD}}(\boldsymbol{G})$ is unmodified, but may now be sampled at many more points.

For some of our structure the atoms do not have identical environments, and the previous approach needs some modification. For the graphite structure, there are two

distinct types of atomic environment which we may denote A and B. However, all atoms are equally disposed with respect to the x axis and so for any reciprocal lattice vector $\boldsymbol{G}_x$ in the x direction we may rigorously write

$$\rho^{\mathrm{A}}_{\mathrm{ALD}}(\boldsymbol{G}_x) = \rho^{\mathrm{B}}_{\mathrm{ALD}}(\boldsymbol{G}_x)\,. \tag{4}$$

Solution of equation (3) now proceeds as before.

For both the FCC slab and the square slab, we have atoms which, although inequivalent with respect to the x axis, are equivalent with respect to y and z. For reciprocal lattice vectors in the yz plane we may therefore proceed as above. For reciprocal lattice vectors in the x direction we proceed as follows. Consider first the square slab: Denoting the atom on the lower layer (with x coordinate 0.0) as A and that on the upper layer as B we have, for some $\boldsymbol{G}_x$,

$$\rho(\boldsymbol{G}_x)V = \rho^{\mathrm{A}}_{\mathrm{ALD}}(\boldsymbol{G}_x) + \rho^{\mathrm{B}}_{\mathrm{ALD}}(\boldsymbol{G}_x)\mathrm{e}^{\mathrm{i}\boldsymbol{R}^{\mathrm{B}}\cdot\boldsymbol{G}_x}\,. \tag{5}$$

If we now slightly raise the upper atom to new position $\boldsymbol{R}^{\mathrm{B}}_{\mathrm{new}}$ whilst retaining the dimensions of our supercell and iterate to charge self-consistency, we will generate a new value $\rho'(\boldsymbol{G}_x)$ for the same $\boldsymbol{G}_x$ component of the charge density. If the displacement is very small then we may assume that the ALDs of atoms A and B are unchanged, and hence

$$\rho'(\boldsymbol{G}_x)V = \rho^{\mathrm{A}}_{\mathrm{ALD}}(\boldsymbol{G}_x) + \rho^{\mathrm{B}}_{\mathrm{ALD}}(\boldsymbol{G}_x)\mathrm{e}^{\mathrm{i}\boldsymbol{R}^{B}_{\mathrm{new}}\cdot\boldsymbol{G}_x}\,. \tag{6}$$

Equations (5) and (6) may be solved simultaneoulsy to yield the required ALD data. Data for the FCC slab and for the diamond structure are obtained by the same procedure.

Having discussed at length our inversion procedure, we turn to its results.

2.3. Free atom

The crosses on Figure 1 show the result of our inversion procedure for the self-consistent charge density of our free-atomic structure. Although data is only available at those values of G corresponding to reciprocal lattice vectors of the system, the smoothness of the plot indicates that data at intermediate points could be found by interpolation. In order to facilitate this interpolation, we have sought to find a good analytical fit for the data. Guided by the form of the pseudopotential we have tried the form,

$$\rho_{\mathrm{AT}}(G) = \frac{3k^2}{(R+A)(k^2+G^2)}[A\cos(GR) + G^{-1}\sin(GR)]\mathrm{e}^{-\beta G^2} \tag{7}$$

with $R = 0.725$ Å, $A = 0.416$, $k = 1.75$ Å^{-1} and $\beta = 0.022$ Å^2 we find an excellent fit shown as the bold line on figure 1.

The magnitude of $\rho_{\mathrm{AT}}(G)$ is fairly negligible for all $G > 3$ Å^{-1}. Therefore only a very small range of G corresponds to appreciable charge density. The importance of this will become apparent later.

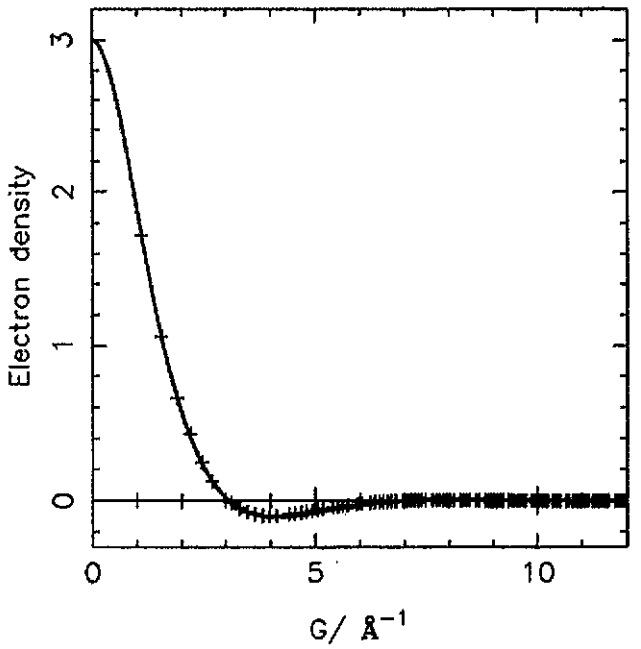

Figure 1. The electron density of a free aluminium pseudo-atom in reciprocal space as a function of wave number (+) and analytic fit to these data (full curve).

2.4. Bulk structures

Four of our 11 structures in table 1 may be described as bulk structures. They are the Face-centred cubic, the vacancy lattice, the simple cubic and the diamond structures. For these structures, and for the unit cells given in table 1, the smallest reciprocal lattice vectors with non-vanishing structure factors are relatively large. The information that could be obtained regarding the ALDs of these structures would therefore be limited to relatively small wavelengths. To overcome this problem we have adopted the procedure outlined in section 2.2. We use the modified supercells of table 2. For three of the structures this involves the construction of large supercells, for the diamond structure it involves distortion of atoms within the same unit cell and solution by the method of equations (5) and (6).

The results of this procedure are plotted in figure 2. For the diamond structure the A and B atoms are almost equivalent and their average has been plotted. In order to facilitate comparison we have also plotted the fitted atomic data of equation (7). The first thing to notice about these points, is that they lie reasonably close to the curve representing the pseudo-atomic data. That is, for this wide range of bulk structures, the self-consistent electron density is at least approximately representable by a simple superposition of identical components, and that these components are very similar to the pseudo-atom density.

On closer inspection we note that for each of these structures, the value of the ALD at low G lies above that of the pseudo-atom data. The curvature of $\rho(G)$ at low G is proportional to the second moment of the real space charge density. We therefore conclude that for these structures, the real space ALDs are contracted relative to that of the pseudo-atom. This result is in agreement with previous work [12], and is also predicted by the effective medium theory [2].

Table 2. Lattice parameters and atomic coordinates for the four distorted aluminium structures.

Structure	a (Å)	b (Å)	c (Å)	Atomic coordinates
Distorted FCC	8.0610	4.0305	4.0305	(0.00, 0.00, 0.00) (0.24, 0.50, 0.00) (0.24, 0.00, 0.50) (0.00, 0.50, 0.50) (0.50, 0.00, 0.00) (0.76, 0.50, 0.00) (0.76, 0.00, 0.50) (0.50, 0.50, 0.50)
Distorted vacancy lattice	8.0610	4.0305	4.0305	(0.24, 0.50, 0.00) (0.24, 0.00, 0.50) (0.00, 0.50, 0.50) (0.76, 0.50, 0.00) (0.76, 0.00, 0.50) (0.50, 0.50, 0.50)
Distorted diamond	2.8500	2.8500	2.8500	(0.00, 0.00, 0.00)
Diamond	6.5817	4.6540	4.6540	(0.00, 0.00, 0.00) (0.24, 0.51, 0.00) (0.51, 0.51, 0.51) (0.76, 0.00, 0.51)
Distorted diamond II	6.5817	4.6540	4.6540	(0.000, 0.000, 0.000) (0.240, 0.508, 0.000) (0.505, 0.505, 0.505) (0.760, 0.000, 0.508)
Distorted simple cubic	11.4000	2.8500	2.8500	(0.00, 0.00, 0.00) (0.24, 0.00, 0.00) (0.50, 0.00, 0.00) (0.76, 0.00, 0.00)

A number of values of G are common to more than one of our structurs. At these values of G we may directly compare the ALDs for the different structures. Differences of 0.1 electron are typical, with differences of up to 0.2 electron occurring for certain values of G. The differences between the ALDs of the different structures appear to follow no apparent pattern.

For some structures we have symmetrically unrelated reciprocal lattice vectors which have the same value of G. Comparison of the data for these points allows assessment of the degree of anisotorpy in the ALD. The spreads in this case are no smaller than those between different structures. Differences of around 0.1 electron are still typical.

In conclusion, the ALDs for these structures qualitatively resembles the pseudo-atomic density. For each structure there are important anisotropies, whilst the variations between different structures are significant and follow no apparent pattern.

2.5. Surfaces

The atoms in a bulk structure are characterized by a relatively isotropic environment. We now turn to structures in which the atomic environment is strongly anisotropic. In the previous section we found that for bulk structures, the self-consistent density at least qualitatively resembled a superposition of pseudo-atomic densities. How must

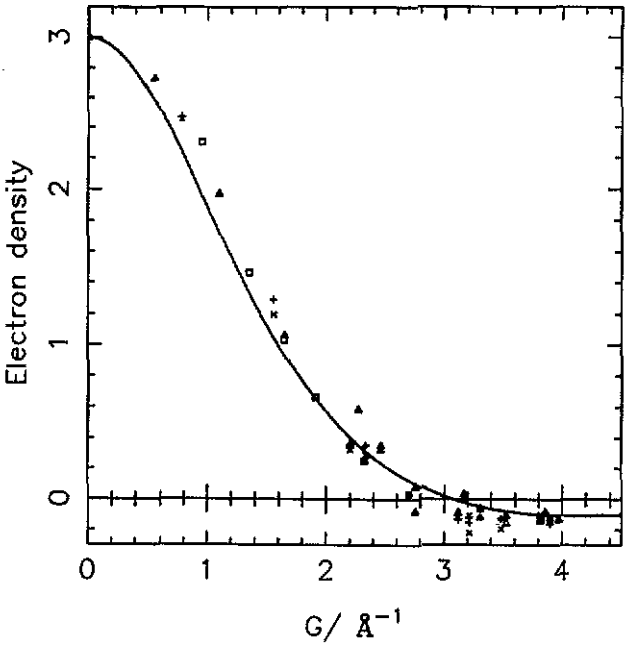

Figure 2. The atomic-like densities in reciprocal space for four aluminium bulk structures. Face-centred cubic (+), Vacancy lattice (×), diamond (□) and simple cubic (△). Full curve shows a fitted form to the electron density of a free aluminium pseudo-atom.

this picture be modified for surfaces?

In order to investigate this, we have taken the remaining six structures of table 1. Five of them are surface-like, the remaining one linear. We have resolved the corresponding self-consistent densities into atom-like components. For three of these structures, all the constituent atoms are equivalent and the procedure is trivial. For one of them, graphite, all the atoms are equivalent with respect to the x axis. We use equation (4) to obtain $\rho_{\mathrm{ALD}}(G_x)$ and ignore all G lying in the yz plane.

For the FCC slab and the square slab, all atoms are equivalent for reciprocal lattice vectors lying within the planes of atoms, so for G in these directions we use equation (4). To obtain data for values of G perpendicular to the surface, we slightly distort our upper layer of atoms, and solve using equations (5) and (6). The results of this procedure are displayed in tables 3 and 4. The significant imaginary part of the electron density is due to the abence of inversion symmetry in the atomic environment.

Table 3. The atomic-like densities of A and B atoms as a function of G_x for the square slab.

G (Å)	$\rho^{\mathrm{A}}_{\mathrm{ALD}}(G)$	$\rho^{\mathrm{B}}_{\mathrm{ALD}}(G)$
0.735	2.394 + 0.034i	2.394 − 0.034i
1.470	1.384 + 0.067i	1.384 − 0.067i
2.204	0.420 + 0.103i	0.420 + 0.103i
2.940	−0.007 − 0.045i	−0.007 + 0.045i
3.674	−0.062 − 0.045i	−0.062 + 0.045i

Table 4. The atomic-like densities of A and B atoms as a function of G_x for the FCC slab.

G (Å)	$\rho^{A}_{ALD}(G)$	$\rho^{B}_{ALD}(G)$
0.855	2.159 + 0.068i	2.159 − 0.068i
1.710	0.954 + 0.011i	0.954 − 0.015i
2.566	0.189 + 0.047i	0.192 − 0.045i
3.421	−0.098 + 0.001i	−0.099 − 0.001i

In order to test the validity of our assumption that our small displacements of the ions around does not significantly affect the atomic-like densities, we have calculated $\rho^{A}_{ALD}(G_x)$ and $\rho^{B}_{ALD}(G_x)$ for the square slab using a less distorted structure than that in table 2. The values obtained agree with those in table 3 to within 0.01 electrons demonstrating the validity of the assumption and the reliability of our results.

The results for the six structures are shown in figure 3. For the two-slab structures we have plotted the real part of the electron density. Given the relative magnitude of the real and imaginary parts, the neglect of the imaginary part is reasonable. Again the points lie around the line representing the pseudo-atomic data. In spite of the strongly inhomogeneous environment of atoms in these structures, it is still possible to represent approximately these self-consistent electron densities as a superoposition of atomic-like densities.

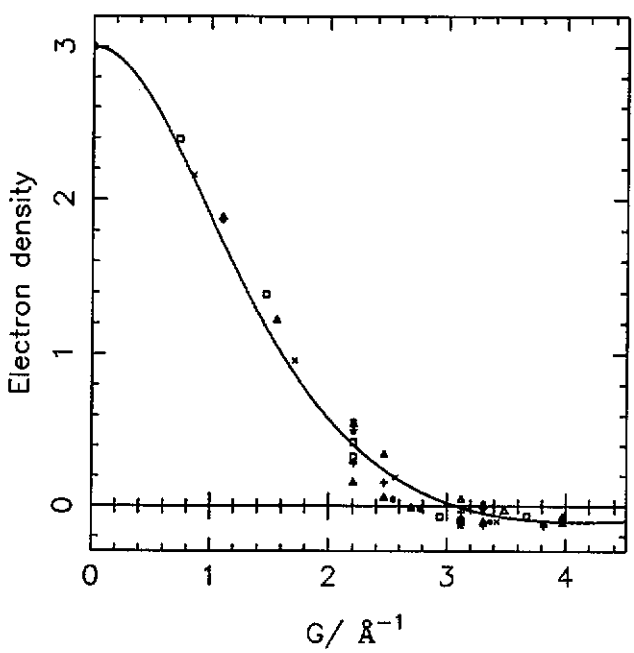

Figure 3. The atomic-like densities in reciprocal space for six aluminium structures. Face-centred cubic slab (×), square slab (□), graphite layer (*), close-packed layer (●), square layer (+) and line (△). Full curve shows a fitted form to the electron density of a free aluminium pseudo-atom.

The data points at low values of G lie somewhat above the pseudo-atomic curve although not as much as was the case for the bulk structures. Again the real space

ALDs for these structures are somewhat contracted relative to that of the free pseudo-atom. We attribute the smaller contraction to the fact that a free-atomic environment resembles much more closely that of an atom at a surface than an atom in bulk.

The spread in the values of the ALDs for those values of G shared by more than one structure is larger than that for bulk structures. The degree of anistropy displayed in the ALDs is also larger, hardly surprising given the greater anisotropy of the structures concerned.

3. The form of the Harris energy surface

3.1. Introduction

In the previous section we established that the self-consistent densities of a wide range of structures can be resolved into atomic-like components which are broadly isotropic and not too different from the electron density of the free pseudo-atom. However, some anisotropies were present, as were deviations in these ALDs from structure to structure. To model all of these densities using a simple spherical density would therefore necessarily introduce certain errors in the electron density. Given that one of our aims is to assess the feasibility of non-self-consistent total energy calculation, it is necessary to determine how these errors in the electron density would translate into errors in total energy. This is the purpose of this section.

3.2. Some properties of the Harris–Foulkes functional

The Harris energy functional introduced separately by Harris and Foulkes [9, 10] is defined as

$$H = \sum_i \varepsilon_i w_i - E_H[n_{in}(r)] + E_{xc}[n_{in}(r)] - \int d^3r\, \mu_{xc}[n_{in}(r)]n_{in}(r) + E_{nn} \qquad (8)$$

where E_H is the Hartree energy, E_{xc} is the exchange-correlation energy, E_{nn} is the nuclear-nuclear interaction, μ_{xc} is the exchange correlation potential, ε_i is the ith eigenvalue and w_i is the corresponding occupation probability.

At the self-consistent electron density, the Harris–Foulkes functional is stationary and gives the correct ground state energy. For input densities sufficiently close to the correct density, errors in the energy are second-order with respect to the errors in the electron density. For some time it was thought that at the correct electron density the functional was a local maximum. It is now known that this is not true [13] and that within the local density approximation the functional is in fact either a saddle-point or a local minimum.

For the special case of nearly uniform systems, rather more about the functional is known [13]. A critical value of G, namely G_c, which is related to the average electron density of the system, may be calculated. For errors in the charge density in Fourier components with $G < G_c$ the functional shows large negative errors. For errors in the charge density in Fourier components such that $G > G_c$ the functional shows errors which are positive and somewhat smaller. Errors in different Fourier components of the electron density produce errors in the energy which are additive. That is, the error in the energy produced by the perturbation of two distinct Fourier components is equal to the sum of the errors induced by performing the perturbations separately.

Most of our structures are rather non-uniform, and it would be unwise simply to apply these results for nearly-uniform systems. We therefore want to study the shape of the Harris functional around the self-consistent density for our 11 structures. Unfortunately, for those structures whose supercells contain large amounts of vacuum many perturbations lead to regions of space with negative electron density. Even those perturbations which do not, can produce rather anomalous behaviour in the Harris–Foulkes functional [22]. For this reason we have restricted our survey to the four bulk structures. Our method is as follows.

For each structure we take the self-consistent electron density. We select a star of Fourier components and perturb each by an amount equal to one electron divided by the square root of the multiplicity of that star. We thereby ensure that the perturbation is properly normalized. This new density is then used to evaluate the Harris–Foulkes energy functional. The procedure is repeated for a number of stars.

Our results are displayed in table 5 and in figure 4. The first thing that to notice is that the form of the results for the different structures are rather similar. That is, in each case we can identify a critical value of G_c marking the boundary between those perturbations which produce negative errors in the energy and those which produce positive errors. Assuming uniformity and ignoring electron correlation, we may calculate G_c as

$$G_c = An^{1/3} \tag{9}$$

where $A = 6.19$ and the electron density n is measured in electrons per cubic angstrom. For each structure we have evaluated G_c. We find for the FCC, the vacancy lattice, the simple cubic and the diamond structures the values of G_c are equal to 3.52 $Å^{-1}$, 3.20 $Å^{-1}$, 3.13 $Å^{-1}$ and 2.71 $Å^{-1}$ respectivley. Inspection of table 5 reveals these values to be in reasonable agreement with our results. They are in each case a little on the high side, reflecting the inhomogeneity of the true electron density and the 1/3 power in equation (9). For each structure, for values of G greater than G_c, the error in the energy is small and saturates. However, for values of G less than G_c the errors in the energy are large and diverge as $1/G^4$.

The relevance of these results for the implementation of non-self-consistent calculations are clear. The Harris–Foulkes functional is not equally sensitive to perturbations of equal magnitude in the electron density. Errors in the electron density at high wavelengths can produce errors which are far greater than perturbations of equal strength at low wavelengths. In constructing an estimate for the self-consistent electron density, it is therefore crucial that the low Fourier components are correct. Some errors in the higher Fourier components are acceptable. It is also clear, that non-self-consistent calculations are far less likely to succeed for systems which possess a large number of small reciprocal lattice vectors with non-zero structure factor.

4. The viability of spherical transferable densities

In section 2 we saw the extent to which the atom-like electron densities which make up the self-consistent densities differed from the pseudo-atomic density. In section 3 we saw the effect which an error in a single star of Fourier components of the charge density has on the energy as calculated by the Harris–Foulkes functional. On the basis of the results of these two sections, we are now in a position to consider the viability of an *a priori* estimate of the electron density based on the superposition of atomic-like densities.

Table 5. The sensitivity of the Harris energy functional to peturbations in the electron density. Errors in the energy are displayed as a function of the magnitude of the Fourier component being perturbed. Perturbation is fixed in magnitude throughout.

	G (Å^{-1})	error in energy (eV)
FCC	1.56	−0.991
	2.21	−0.209
	2.70	−0.044
	3.12	−0.010
	3.47	0.029
	3.82	0.040
	4.41	0.050
	4.68	0.069
	4.93	0.073
	5.17	0.084
Vacancy lattice	1.56	−0.659
	2.21	−0.130
	2.70	−0.008
	3.12	0.036
	3.47	0.089
	3.82	0.096
	4.41	0.090
	4.68	0.134
	4.93	0.163
	5.17	0.143
Simple cubic	0.55	−36.961
	1.10	−3.456
	1.65	−0.615
	2.21	−0.083
	2.76	0.001
	3.31	0.033
Diamond	0.95	−2.386
	1.36	−0.614
	1.66	−0.076
	1.91	−0.058
	2.14	−0.012
	2.33	0.015
	2.70	0.133
	2.86	0.053
	3.30	0.073
	4.67	0.097

4.1. Sphericity

To what extent is it possible to reproduce any self-consistent density by the superposition of spherical densities? Of our 11 structures, only the atomic structure has atoms which are truly spherical. The other structures are all to a lesser or grater extent non-isotropic. In section 2 it was noted that this anisotropy led to variations in $\rho_{\mathrm{ALD}}(G)$ for a given structure and for a given G of up to 0.4 electrons. To represent $\rho_{\mathrm{ALD}}(G)$ by a spherically symmetric function would therefore introduce errors in $\rho_{\mathrm{ALD}}(G)$ of up to 0.2 electrons. In calculating the electron density for the whole system one would sum this error over all components of a star and over all atoms of a unit cell. From what we have learnt in section 3 we would expect the corresponding error in the energy to be fairly significant. In order to find its magnitude, we have

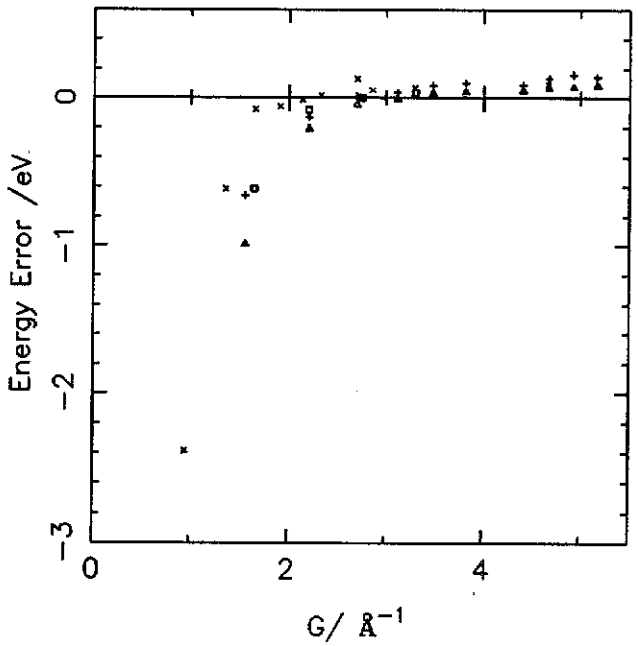

Figure 4. Sensitivity of the Harris functional to peturbations in the electron density. Errors in the energy are shown as a function of the magnitude of the Fourier component being perturbed. In each case the magnitude of the perturbation is fixed. Data is shown for the four bulk structures. Face-centred cubic (△), Vacancy lattice (+), diamond (×) and simple cubic (□). Full curve shows a fitted form to the electron density of a free aluminium pseudo-atom.

adopted the following procedure.

For each of our structures in turn, we take the self-consistent density and by the procedure of 2.2 resolve it into atom-like components. We take these ALDs and 'sphericize' them. That is, for each value of G for which we have differing values of $\rho_{\mathrm{ALD}}(\boldsymbol{G})$, we take the average. We now take this sphericized density and use it as an input density to calculate the energy of the structure from which it was derived. The results of this procedure together with the correct self-consistent energies, are displayed in table 6.

For many of our structures the energy difference is small, due in part to the near-sphericity of the constituent atomic environment. However, an equally important reason is undoubtedly that for our structures, very few reciprocal lattice vectors not related by symmetry possess the same magnitude. We note that if the x and y dimensions of the linear structure had not been precisely in the ratio 2:1, then the energy difference in sphericizing would have been significatnly reduced.

Allowing for this, the energy differences for the linear, diamond and square structure of 0.03 eV, 0.01 eV and 0.01 eV respectively should not be regarded as anomalous. It is possible that the positive and negative errors which arose due to the neglect of anisotropy cancel. However it would be dangerous to rely on such a cancellation, and we conclude that an energy error of around 0.02 eV per atom is an upper bound on the reliability of any method which relies on the superposition of spherical densities.

Table 6. Effect of charge anisotropy on energies of the 11 structures. Column 1 shows correct electron density. Column 2 shows result of using 'sphericized' electron density.

Structure	Energy per atom	
	E_0 (eV)	E_1 (eV)
FCC	−58.287	−58.287
Vacancy lattice	−58.072	−58.072
Simple cubic	−57.885	−57.885
Diamond	−57.371	−57.359
Atom	−54.909	−54.909
Line	−56.236	−56.203
Square lattice	−57.255	−57.247
Close-packed layer	−57.453	−57.452
Square slab	−57.590	−57.592
FCC slab	−57.817	−57.817
Graphite	−56.883	−56.882

4.2. Transferability

The previous section has shown that the restriction of spherical ALDs is likely to result in errors in the total energies of up to 0.03 eV per atom. To the extent that the ALDs in some of the structures are more spherical than in others, it should be already clear that there is no universal ALD that will describe adequately all structures. However we should also like to know what additional differences there are between the atom-like densities which make up the different structures. That is, how do the spherically averaged atom-like densities differ from structure to structure, and is it possible to introduce a universal spherically symmetric density which yields errors in the energy no greater than those of the previous section.

In order to investigate this, we have taken the fitted pseudo-atomic charge density of equation (7) and have used it as the input density to calculate the energy of our 11 structures. Our results are shown in the first column of table 7. The errors range from 0.003 to 0.253 eV per atom, being smallest for the bulk and largest for the surface structures. From considerations in sections 2 and 3 we tentatively attribute this to three factors. Firstly there is the greater sensitivity of the Harris functional to errors in the electron density at low G, secondly there are errors in the electron densities which are generally larger for smaller G and lastly the bulk structures have fewer reciprocal lattice vectors at small G.

In order to support this interpretation, we adopt the following procedure. The self-consistent charge density of each structure is taken in turn. For each reciprocal lattice vector $G > 3$ Å^{-1} we then replace the self-consistent charge by that given by equation (7) i.e. the corresponding value of equation (7) multiplied by the structure factor for that value of G. This new charge density is now used to calculate an estimate for the energy of the structure. The results of this procedure are displayed in the second column of table 7. We now repeat the procedure but this time perturb only those components such that $G < 3$ Å^{-1}. The results of this procedure are displayed in the final column of table 7. Comparison of the columns of table 7 separate out the effect on the energy of those errors in low Fourier components and those errors in high

Fourier components. As expected, those errors in the low Fourier components produce large negative errors in energy, whilst those at high G tend to produce a positive and somewhat smaller error.

Table 7. Viability of transferrable atomic-like density. Column 1 shows energies of the 11 structures using the pseudo-atomic ensity. Column 2: as above but using pseudo-atomic density only for those Fourier components with $G < 3$ Å. Column 3: as above but only using pseudo-atomic density for those Fourier components with $G > 3$ Å.

	Energy per atom		
Structure	E_0 (eV)	E_1 (eV)	E_2 (eV)
FCC	−58.305	−58.285	−58.298
Vacancy lattice	−58.118	−58.062	−58.116
Simple cubic	−57.880	−57.871	−57.887
Diamond	−57.368	−57.339	−57.362
Atom	−54.899	−54.903	−54.904
Line	−56.381	−56.212	−56.360
Square lattice	−57.410	−57.241	−57.405
Close-packed layer	−56.626	−57.432	−57.620
Square slab	−57.709	−57.568	−57.707
FCC slab	−58.070	−57.809	−58.067
Graphite	−57.048	−56.840	−57.008

We conclude that smaller errors in the bulk calculations are purely an artifact of the small number of low reciprocal lattice vectors that these structures posses. They are in no way an indication that the atom-like charges in bulk structures particularly resemble that of the free pseudo-atom.

The errors in the energy in table 7 are rather large. Inspection of figures 2 and 3 suggests that these errors could be reduced by using an electron density similar to that of equation (7) but somewhat dilated in reciprocal space. In order to find such a density we have taken the low G data of figures 2 and 3 and again using the functional form of 7 performed a least-squares fit. We find new values $R = 0.725$ Å, $A = 0.316$, $k = 1.91$ Å^{-1} and $\beta = 0.012$ Å^2. The new fit is shown in figure 5. We take this new density and use it to calculate the energy of 11 structures, with the results shown in table 8. Although the error for some of the structures has been increased (particularly that for the atom), the overall agreement is better. The errors for the surfaces are reduced by around 75% and the maximum error is reduced from 0.253 eV to 0.079 eV per atom. All of the energy errors are negative and of similar magnitude. As a consequence the energy differences between structures other than the atomic, show errors of around 0.01 eV per atom, with the smallest being 0.01 eV and the largest 0.054 eV.

5. Conclusion

We have shown that it is at least qualitatively reasonable to consider the self-consistent charge density of a large number of structures to be composed of the superposition of

Table 8. Energy of the 11 structures using optimized atomic-like electron density.

Structure	Energy using modified atomic density (eV per atom)
FCC	−58.339
Vacancy lattice	−58.121
Simple cubic	−57.932
Diamond	−57.396
Atom	−55.001
Line	−56.267
Square lattice	−57.314
Close-packed layer	−57.506
Square slab	−57.652
FCC slab	−57.896
Graphite	−56.933

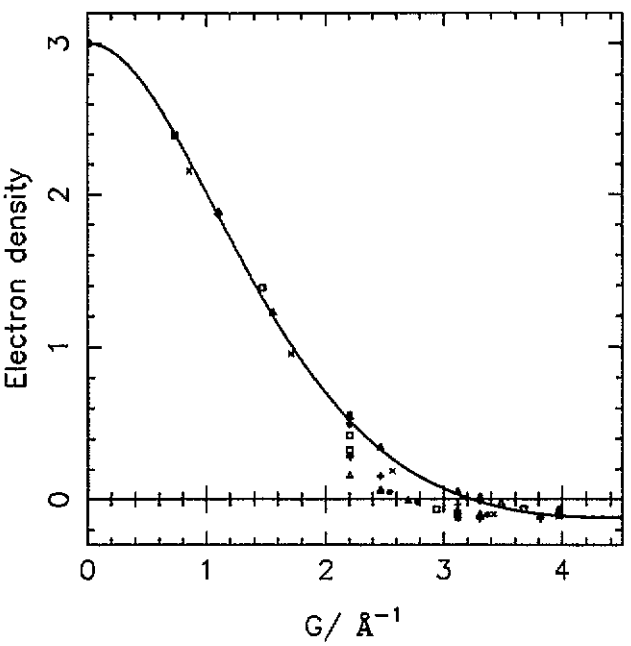

Figure 5. The atomic-like densities in reciprocal space for six aluminium structures. Face-centred cubic slab (×), square slab (□), graphite layer (*), close-packed layer (●), square layer (+) and line (△). Full curve shows least-squares fit to the data at low G.

atom-like entities. These entities are very similar to the true pseudo-atomic density but slightly dilated in reciprocal space, i.e. contracted in real space.

Anisotopy in the local environment generates significant anisotropy in the electron density. Consequently, any estimate of the electron density based on the superposition of spherical entities is likely to yield errors of around 0.02 eV per atom.

Use of the pseudo-atomic density in the 10 structures besides the free atom, yields errors in the energy of up to −0.253 eV per atom. The errors are principally due to a negative contribution from errors in the low Fourier components of the electron density. For our bulk structures which hve very few low reciprocal lattice vectors the errors in energy are inevitably less, although this would not be the case for amorphous structures.

We have found a single spherical density which correctly yields the energy of our 10 non-atomic structures to within 0.079 eV per atom. Energy differences are mostly correct to within 0.01 eV per atom, the worst case being 0.054 eV per atom.

Since errors in an electron density can result in both positive and negative errors in energy, it is possible for less accurate electron densities to give more accurate energies. However this error cancellation is fortuitious, and it is not possible to rely on this effect. We conclude that the energy errors stated here are an upper bound on the reliability of any non-self-consistent scheme.

Acknowledgments

The authors thank the Science and Engineering Research Council for a studentship (IJR) and for use of the CRAY XMP at the Rutherford Appleton Laboratory under grant GR/E 91790. One of us (MCP) thanks the Royal Society for financial support.

References

[1] Godby R, Needs R J and Payne M C 1990 *Phys. World* 3 39
[2] Jacobsen K W, Norskov J K and Puska M J 1987 *Phys. Rev.* B 35 7423
[3] Ercolessi F, Parrinello M and Tosatti E 1988 *Phil. Mag.* A 58 213
[4] Foiles S M, Baskes M I and Daw M S 1986 *Phys. Rev.* B 33 7983
[5] Pettifor D G 1989 *Phys. Rev. Lett.* 63 2480
[6] Finnis M W and Sinclair J E 1984 *Phil. Mag.* A 50 45
[7] Sutton A P, Finnis M W, Pettifor D G and Ohta Y 1988 *J. Phys. C: Solid State Phys.* 21 35
[8] Kohn W and Sham L J 1965 *Phys. Rev.* A 140 1133
[9] Foulkes M and Haydock R 1989 *Phys. Rev.* B 39 12520
[10] Harris J 1985 *Phys. Rev.* B 31 1770
[11] Read A J and Needs R J 1989 *J. Phys.: Condens. Matter* 1 7565
[12] Finnis M W 1990 *J. Phys.: Condens. Matter* 2 331
[13] Robertson I J and Farid B 1991 *Phys. Rev. Lett.* 66 3265
[14] Robertson I J, Payne M C and Heine V 1991 *Europhys. Lett.* 15 301
[15] Car R and Parrinello M 1985 *Phys. Rev. Lett.* 55 2471
[16] Heine V 1991 *Solid State Physics* vol 35 (New York: Academic) pp 80–82
[17] Goodwin L, Needs R J and Heine V J 1990 *J. Phys.: Condens. Matter* 2 351
[18] Ceperley D M and Alder B J 1980 *Phys. Rev. Lett.* 45 566
[19] Perdew J P and Zunger A 1981 *Phys. Rev.* B 23 5048
[20] Robertson I J and Payne M C 1990 *J. Phys.: Condens. Matter* 2 9837
[21] Monkhorst J J and Pack J D 1976 *Phys. Rev.* B 13 5188
[22] Robertson I J *et al* in preparation